BIOCHEMISTRY
including biophysical chemistry & molecular biology

Article

pubs.acs.org/biochemistry

The αA66−80 Peptide Interacts with Soluble α-Crystallin and Induces Its Aggregation and Precipitation: A Contribution to Age-Related Cataract Formation

Rama Kannan,[†] Puttur Santhoshkumar,[‡] Brian P. Mooney,[§] and K. Krishna Sharma*[,†,‡]

[†]Department of Biochemistry, University of Missouri, Columbia, Missouri 65211, United States

[‡]Department of Ophthalmology, University of Missouri School of Medicine, Columbia, Missouri 65212, United States

[§]Charles W. Gehrke Proteomics Center, University of Missouri, Columbia, Missouri 65211, United States

Supporting Information

ABSTRACT: Formation of protein aggregates in the aging eye lens has been shown to correlate with progressive accumulation of specific low-molecular weight (LMW) peptides derived from crystallins. Prominent among the LMW fragments is αA66−80, a peptide derived from αA-crystallin and present at higher concentrations in the water-insoluble nuclear fractions of the aging lens. The αA66−80 peptide has amyloid-like properties and preferentially insolubilizes α-crystallin from soluble lens fractions. However, the specific interactions and mechanisms by which the peptide induces α-crystallin aggregation have not been delineated. To gain insight into the mechanisms of peptide-induced aggregation, we investigated the interactions of the peptide with α-crystallin by various biochemical approaches. The peptide weakens α-crystallin chaperone ability and drastically promotes α-crystallin aggregation via the formation of insoluble peptide−protein complexes through transient intermediates. 4,4′-Dianilino-1,1′-binaphthyl-5,5′-disulfonic acid studies suggest that the peptide induces changes in the hydrophobicity of α-crystallin that could trigger the formation and growth of aggregates. The peptide−α-crystallin aggregates were found to be resistant to dissociation by high ionic strengths, whereas guanidinium hydrochloride and urea were effective dissociating agents. We conclude that the αA66−80 peptide forms a hydrophobically driven, stable complex with α-crystallin and reduces its solubility. Using isotope-labeled chemical cross-linking and mass spectrometry, we show that the peptide binds to multiple sites, including the chaperone site, the C-terminal extension, and subunit interaction sites in αB-crystallin, which may explain the antichaperone property of the peptide and the consequential age-related accumulation of aggregated proteins. Thus, the α-crystallin-derived peptide could play a role in the pathogenesis of cataract formation in the aging lens.

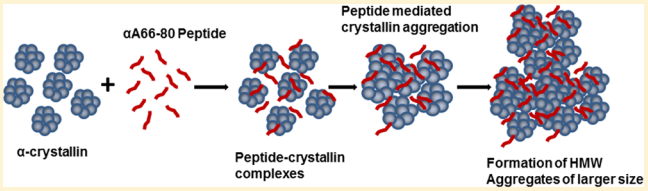

Age-related cataract is common and causes a huge economic burden. Cataract is characterized by increasing cloudiness of the lens and progressive loss of vision caused by the formation of protein aggregates.[1] The formation of peptide and/or protein aggregates is associated with the pathogenesis of numerous debilitating human diseases, such as Alzheimer's disease, systemic amyloidosis, and Parkinson's disease.[2] The underlying processes behind the development of these protein aggregation disorders are unclear. A similar unexplained phenomenon operates behind the development of protein aggregation in lens. Multiple factors such as age-related modifications of lens proteins, oxidative stress, and other conditions are believed to be involved, but how they influence the rate and extent of protein aggregation remains unknown.

Lens transparency relies on the solubility and stability of lens proteins, called crystallins, of which there are of three types: α-, β-, and γ-crystallins. α-Crystallin, a small heat shock protein, is the most abundant of lens proteins and is composed of two subunits, αA and αB, each 20 kDa. α-Crystallin subunits oligomerize to a polydisperse protein with an average molecular mass of 800 kDa.[1] α-Crystallin has chaperone activity[3] and is responsible for suppressing the aggregation of other lens proteins. The chaperone activity of α-crystallin and the molecular interactions among the crystallins are responsible for maintaining lens transparency and the appropriate refractive index.[3,4] Progressive age-related loss of lens transparency and cataract formation has been attributed to various post-translational modifications in lens proteins. These modifications include deamidation, oxidation, methylation, phosphorylation, and truncation. Racemization of Ser, Thr, Glu/Gln, and Phe in lens proteins has recently been reported in aged and cataract lenses.[5] With these changes, aged lens proteins exhibit decreased chaperone activity, altered stability, and decreased solubility, resulting in the formation of high-molecular weight (HMW) aggregates.[6,7] The most notable change observed in the aging lens is the progressive degradation of crystallins.[8,9] In human lens, the quantity of degraded crystallins increases with the severity of cataract. Increased quantities of truncated

Received: December 14, 2012
Revised: April 29, 2013
Published: April 30, 2013

crystallins and LMW peptide fragments are present in the water-insoluble aggregates of aging and cataract lenses.[10−12] A decreased rate of clearance of peptide fragments by peptidases or an increased level of proteolysis has been implicated in the accumulation of peptide fragments in the aging lens. It is not known whether cleavage of crystallins to LMW peptides is an important step in the process of age-related cataract formation or is a normal event in the degradation of crystallins.

The release of peptide fragments from native proteins as a result of abnormal proteolysis of host proteins is a major contributing factor in the pathogenesis of various neurodegenerative diseases.[13] In such diseases, specific peptide fragments that remain part of the three-dimensional conformation in native proteins do not have aggregation potential, but when peptide fragments become cleaved and released, they exhibit a propensity to aggregate and a tendency to influence the stability and aggregation behavior of proteins.[14] Thus, the age-related appearance of peptide fragments and associated protein aggregation in the lens has led to the emerging hypothesis that peptides could be the initiating factor or a facilitating factor in protein aggregation and cataract formation. This hypothesis has become significant for the following reasons. First, aging and cataract lenses show increased levels of proteolysis compared to those of age-matched noncataract lenses.[15,16] Second, the crystallin fragments are largely found colocalized with aggregates in the opaque region of the lens as compared to the clear region of the same lens.[8,11,12,15,16] Third, peptides have interaction sites in soluble crystallins and are found to modulate the normal physiology of the lens.[17] For example, an oxidized peptide from βB3-crystallin has been shown to increase the level of aggregation of both β- and γ-crystallins.[18] Moreover, peptides have been found to suppress the chaperone ability of α-crystallin, increase the oligomeric size of soluble crystallin,[11,19] interact tightly with cytoskeletal and membrane components, alter the interaction of soluble α-crystallin with the membrane,[20,21] and form amyloid-type aggregates *in vitro*.[19,22] Such aberrant interactions with soluble proteins and cellular components are the characteristic features of pathological peptides such as p25, β-amyloid, and polyglutamine fragments as well as the synthetic peptides with amyloidogenic potential.[13,23,24]

A degradation product of αA-crystallin, ^{66}SDRDKFVIFLDVKHF^{80} (αA66−80), is prominent among the LMW crystallin fragments (<3.5 kDa) that accumulate in the aging lens (Figure 1). We have characterized the lens distribution, properties, and

```
 1 MDVTIQHPWFKRTLGPFYPSRLFDQFFGEGLFEYDLLPFLSSTISPYYRQSLFRTVLDSG  60

                 αA66-80
61 ISEVRSDRDKFVIFLDVKHFSPEDLTVKVQDDFVEIHGKHNERQDDHGYISREFHRRYRL 120

121 PSNVDQSALSCSLSADGMLTFCGPKIQTGLDATHAERAIPVSREEKPTSAPSS 173
```

Figure 1. αA-Crystallin sequence showing the αA66−80 peptide regions and chaperone site. Red denotes residues 66−80. The underlined sequence is the chaperone site in αA-crystallin.

aggregation potential of this peptide.[19] The αA66−80 peptide is derived from the chaperone site in αA-crystallin[25] and has regions homologous to the Aβ(1−42) peptide, which is responsible for its polymerizing properties.[26] The αA66−80 peptide preferentially insolubilizes α-crystallin from soluble lens crystallins composed of α-, β-, and γ-crystallins. The peptide-induced α-crystallin aggregates serve as seeds for further aggregation with other soluble proteins.[19] These attributes, combined with the observation that the αA66−80 peptide is distributed primarily in the WIS fractions from the nuclear region of the human lens,[12,19] provide strong evidence of, and an explanation for, the decrease in the level of soluble α-crystallin with aging, especially in the lens nucleus and to a greater extent in the cataractous lens.[27,28] Thus, it is probable that the αA66−80 peptide plays a critical role in crystallin aggregation and cataract formation. However, the mechanisms underlying the generation of the peptide in the lens are yet to be elucidated, including the α-crystallin sequences involved in interactions with the αA66−80 peptide and how the peptide induces aggregation of soluble α-crystallin. To gain insights into the effect of the accumulating αA66−80 peptide on α-crystallin structure and function, we have investigated α-crystallin aggregation in the presence of the αA66−80 peptide. In this study, we show a direct interaction between the peptide and α-crystallin subunits as well as the possible mechanism underlying peptide-induced aggregate formation. We identified the peptide interaction regions in αB-crystallin using a novel cross-linker. We found that the peptide suppresses α-crystallin chaperone activity, decreases the solubility of α-crystallin, and increases the surface hydrophobicity in α-crystallin by forming stable noncovalent interactions with α-crystallin. Additionally, we describe the *in vitro* effects of the peptide on α-crystallin and discuss the potential impact of αA66−80 in initiating or facilitating aggregation in lens. Our findings enhance our understanding of the mechanisms of protein aggregation in cataract formation, which may influence therapeutic strategies to prevent or delay the onset of cataract.

MATERIALS AND METHODS

Materials. Synthetic peptides, ^{66}SDRDKFVIFLDVKHF^{80} (αA66−80), ^{43}TISPYYRQSLFRTV^{56} (αA43−56), SDRDKFVIFLDVKHFK-Biotin (C-terminally biotinylated αA66−80), SDRDKF**P**IFLDVKHF (proline-substituted αA66−80), and EEKPAVTAAPK (C-terminal peptide of αB-crystallin), were obtained from Genscript Corp. The purity of the synthetic peptide exceeded 95%. The lyophilized peptide (2 mg) was dissolved in sterile water at a concentration of 5 mg/mL, sonicated for 10 s, filtered through a 0.2 μm filter, and used immediately. The peptide incubations and assays were conducted in phosphate buffer [50 mM sodium phosphate buffer containing 150 mM NaCl (pH 7.2)]. Alcohol dehydrogenase (ADH) was obtained from Worthington Biochemical. The cross-linking reagents BS^{2}G-d_0 and -d_4 [bis(sulfosuccinimidyl) glutarate] were purchased from Proteochem. Bis-ANS (4,4′-dianilino-1,1′-binaphthyl-5,5′-disulfonic acid) was obtained from Sigma-Aldrich. Bovine trypsin (sequencing grade) was obtained from G-Biosciences. Bio-Rad protein assay reagent was used to estimate the protein concentrations in various assays.

Preparation of α-Crystallin. α-Crystallin from bovine lenses was isolated by gel filtration on Sephadex G-200 and ion-exchange chromatography on Q-Sepharose (GE Healthcare Biosciences) as described previously.[29]

Expression and Purification of Recombinant αB-Crystallin. Human αB-crystallin cDNA (obtained from J. Mark Petrash, University of Colorado, Denver, CO) was cloned in a pET23d vector (Novagen) at the NcoI/HindIII site and expressed in *Escherichia coli* BL21(DE3) pLysS cells (Invitrogen). The recombinant protein was purified by a combination of gel filtration (Superdex G-200) and ion-exchange chromatography (Q-Sepharose), as described pre-

dx.doi.org/10.1021/bi301662w | *Biochemistry* 2013, 52, 3638−3650

viously.[30] The purity of the protein was confirmed by sodium dodecyl sulfate−polyacrylamide gel electrophoresis (SDS−PAGE). The recombinant αB-crystallin used for the cross-linking experiments was >95% pure.

Chaperone Assays. The ability of α-crystallin to suppress aggregation of ADH in the presence of the αA66−80 peptide was assessed as described previously.[19] The αA43−56 peptide was used as a control, as this peptide has no aggregation potential.[31] α-Crystallin (50 μg) was incubated with ADH (150 μg) and the αA66−80 or αA43−56 peptide (5 and 15 μg) in 1 mL of 50 mM phosphate buffer containing 50 mM EDTA (pH 7.2). Aggregation was monitored for 120 min by measuring the absorption at 360 nm and 37 °C in a spectrophotometer equipped with a temperature-regulated multicell holder. After the chaperone assay, the samples were centrifuged at 8000 rpm for 15 min. The composition of the pellet was determined by SDS−PAGE.

Aggregation Assays. The susceptibility of the protein to peptide-induced aggregation was evaluated by different means. Samples containing α-crystallin (5 μM) and peptide (25 μM) in 1 mL of 50 mM phosphate buffer were incubated at 37 °C. To assess protein aggregation, the turbidity of 1 mL of the solution was determined spectrophotometrically by measuring the change in absorbance at 360 nm after different periods of incubation. α-Crystallin samples incubated without added peptide were used as a control. The concentration of the soluble α-crystallin remaining in the supernatant as a function of time during incubation was determined by the Bio-Rad assay. In another experiment, α-crystallin (10 μM) was incubated with the peptide (1.25−20 μM) in 1 mL of 50 mM phosphate buffer at 37 °C for 24 h. The samples were then centrifuged at 8000 rpm for 15 min, and pellets were run via SDS−PAGE.

Intrinsic Tryptophan Fluorescence Measurements. The fluorescence spectra of α-crystallin in the presence and absence of the αA66−80 peptide were recorded using a JASCO FP750 spectrofluorometer. α-Crystallin (5 μM) was mixed with increasing concentrations of the peptide (α-crystallin:αA66−80 molar ratios of 1:0, 1:0.25, 1:0.5, 1:1, 1:1.5, and 1:2) in 1 mL of 50 mM phosphate buffer (pH 7.2). The samples were excited at 295 nm, and tryptophan emission spectra were recorded between 300 and 400 nm (bandwidth of 5 nm). All reaction mixtures were incubated for 10 min at 37 °C to reach equilibrium prior to measurements.

Circular Dichroism Measurements. Far-UV circular dichroism (CD) experiments were conducted using a JASCO J-815 spectropolarimeter equipped with a thermostated cell holder. α-Crystallin (5 μM) was mixed with αA66−80 (α-crystallin:αA66−80 molar ratios of 1:0, 1:0.25, 1:0.5, 1:1, 1:1.5, 1:2, and 1:4). Samples taken in 10 mM phosphate buffer (pH 7.2) were incubated at 37 °C for 10 min before far-UV CD measurements. Measurements were acquired in the range of 200−240 nm using a 1 mm path quartz cuvette at 25 °C. All spectra were corrected by subtracting the buffer baseline and appropriate peptide controls. The derived spectrum represents an average of five scans.

Size Exclusion Chromatography (SEC). α-Crystallin (5 μM) was incubated with αA66−80 (α-crystallin:αA66−80 molar ratios of 1:0, 1:0.25, 1:0.5, 1:1, 1:2, and 1:4) in 250 μL of 50 mM phosphate buffer (pH 7.2) at 37 °C for 10 min. Samples were then filtered through a 0.45 μm filter (Millipore). The filtrate (150 μL) was injected onto a TSK G5000PW$_{XL}$ column (Tosoh Bioscience) gel-filtration column connected to a high-performance liquid chromatography (HPLC) system (Shimadzu) equipped with UV and refractive index detectors. Samples were eluted using 50 mM phosphate buffer (pH 7.2), and the elution was monitored at 280 nm.

Bis-ANS Binding Studies. Bis-ANS is an environment-sensitive hydrophobic fluorescent dye. The fluorescence quantum yield of bis-ANS increases when it binds to hydrophobic regions of proteins such as α-crystallin.[32] Bis-ANS (20 μM) was added to α-crystallin (10 μM) incubated with the αA66−80 peptide (α-crystallin:αA66−80 molar ratios of 1:0, 1:0.25, 1:0.5, 1:1, 1:1.5, and 1:2) in 1 mL of 50 mM phosphate buffer (pH 7.2). The samples were thoroughly mixed and incubated for 10 min before measurements were taken. The fluorescence of the bis-ANS bound to α-crystallins incubated in the presence and absence of peptides was measured using a JASCO FP750 spectrofluorometer. The interaction between the C-terminal region of αB-crystallin (EEKPAVTAAPK; αB-CTP) and the αA66−80 peptide was confirmed in a separate experiment. The fluorescence intensity of bis-ANS bound to α-crystallin (100 μg) was measured in the presence of αB-CTP (10 μg) and αA66−80 (10 μg) or proline-substituted αA66−80 (10 μg). Fluorescence emission spectra were recorded from 400 to 600 nm using an excitation wavelength of 390 nm. The excitation and emission slits were set at 5 nm.

Dissociation Studies of α-Crystallin−αA66−80 Complexes. α-Crystallin (200 μg) was incubated with αA66−80 (100 μg) in 500 μL of 50 mM phosphate buffer for 24 h at 37 °C. After centrifugation at 12000 rpm for 30 min, aggregates were suspended in 100 μL of each of the dissociating agents for 1 h while the mixture was being gently stirred at 37 °C (50 mM phosphate buffer containing 1% SDS, 6 M GdmCl, 8 M urea, 1% Tween 20, 1% Triton X-100, 1 M NaCl, and 1 M $MgCl_2$). The redissolved aggregates were then centrifuged at 12000 rpm for 30 min. The soluble protein content of the supernatant fractions of redissolved aggregates was determined by the Bio-Rad protein assay and compared with the protein content of samples that were not incubated.

Cross-Linking Studies. The peptide interaction sites in αB-crystallin were evaluated using chemical cross-linking and mass spectrometry approaches. Isotope-labeled homobifunctional cross-linker *N*-hydroxysuccinimide esters BS^{2}G-d_0 and -d_4 were used in 1:1 mixtures of their nondeuterated (d_0) and deuterated (d_4) species. The reaction mixture containing αB wild-type (WT) crystallin (200 μg) and biotin-labeled αA66−80 (100 μg) [2:1 (w/w)] in 1 mL of 25 mM phosphate buffer (pH 7.4) was incubated at room temperature for 30 min prior to the addition of the cross-linker. An αB-WT crystallin sample without added peptide was used as a control. A 1 M stock solution of BS^{2}G-d_0 and -d_4 cross-linker in DMSO was prepared. A 20-fold molar excess of the cross-linker (1:1 d_0:d_4 ratio) was added to the peptide/protein incubation mixture. Cross-linking reactions were allowed to proceed for 45 min on ice. A control sample containing the protein/peptide mixture without the added cross-linker was maintained. The cross-linking reaction was terminated by adding 50 μL of a Tris (final concentration of 20 μM) solution to each sample. After incubation at room temperature for 10 min, the samples were passed through a 10K centrifugal filter device (Centricon) to remove unreacted cross-linker.

SDS−PAGE, Western Blotting, and Digestion of Cross-Linked Products. The cross-linking reaction mixtures were separated by one-dimensional SDS−PAGE. The resolved samples were transferred to a PVDF membrane and, using

avidin-HRP (Pierce), assayed for the detection of the cross-linked complex of αB-crystallin that is covalently linked with biotinylated αA66−80. Following this, the bands of interest containing the cross-linked product were excised and in-gel-digested using trypsin. The samples were dissolved in trypsin digestion buffer [0.2 M ammonium bicarbonate (pH 7.9)], and 2 μg of bovine trypsin was added to 200 μg of total proteins. After incubation for 2 h, a second batch of trypsin (2 μg) was added to achieve complete digestion. The digestion took place in complete darkness at 37 °C overnight.

Identification of Cross-Linked Products by Liquid Chromatography and Tandem Mass Spectrometry (LC−MS/MS). The extracted peptides were lyophilized and resuspended in 8 μL of 5% acetonitrile and 1% formic acid. Separation of peptides was achieved in two steps. A portion of the digest was loaded onto a C8 trap column (Michrom Bioresources). Eluates were then passed through C18 reversed-phase resin. Peptides were eluted from 5 to 40% acetonitrile (in 0.1% formic acid) over 70 min. Eluted peptides were reversed-phase separated using integrated Proxeon nano-HPLC coupled online to an LTQ-Orbitrap XL spectrometer (Thermo Scientific). Masses were acquired using a high-resolution FTMS scan of the eluting peptides. Postacquisition, the LC−MS experimental peptide mass lists obtained were matched with theoretical mass lists of cross-linked peptides generated using GPMAW (General Protein Mass Analysis for Windows, version 9.2) with the mass tolerance set at 5 ppm. GPMAW allows the user to define the protein and the peptide sequences as well as the homobifunctional amine-reactive cross-linker, BS^2G, used in this study. Amine groups in the protein and peptide were chosen as reactive sites for the cross-linker. With this approach, theoretical peak lists corresponding to peptides cross-linked with light (d_0) and heavy (d_4) precursors were generated. Subsequently, by comparison with the GPMAW-generated possible cross-linked peptides, the m/z values obtained via LC−MS were assigned to cross-linked products. The identified cross-linked peptides (parent ion) from LC−MS were validated by MS/MS analysis. In the second MS spectrum, the parent ion selected is subjected to peptide fragmentation (CID in ion trap and HCD in C-trap) producing the MS/MS spectrum. The b and y ion series resulting from fragmentation along the peptide backbone were interpreted from the low-mass end through to the highest-mass ion. Peptide sequences were confirmed using MASCOT distiller software.

RESULTS

The αA66−80 Peptide Suppresses the Chaperone Activity of α-Crystallin. The ability of α-Crystallin to suppress aggregation of ADH in the presence of peptides was assessed. When native ADH was incubated at 37 °C in the presence of EDTA containing phosphate buffer (50 mM, pH 7.5), ADH unfolded and aggregated into particles sufficiently large to scatter light at 360 nm (Figure 2, curve 1). In contrast, incubation with α-crystallin suppressed aggregation of the ADH in its denatured state because of the α-crystallin chaperone activity (Figure 2, curve 2). Control peptide αA43−56 had no effect on α-crystallin chaperone activity (Figure 2, curves 3 and 4) and did not cause aggregation of samples. The addition of αA66−80 diminished the chaperone activity of α-crystallin and increased in a concentration-dependent manner the level of aggregation and precipitation of α-crystallin and ADH substrate (Figure 2, curves 5 and 6). Additionally, the peptides by themselves did not precipitate and scatter light under the

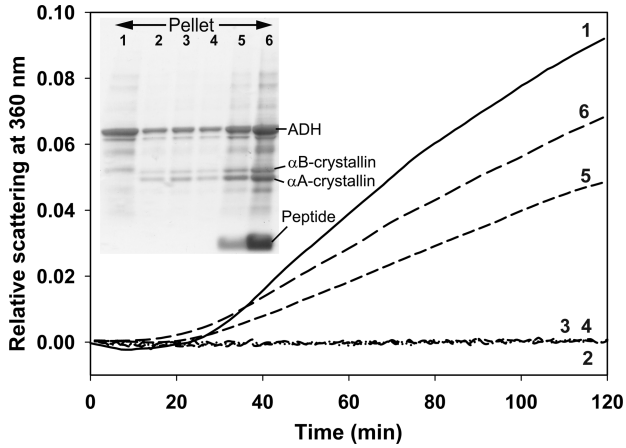

Figure 2. Effects of the αA66−80 peptide on the chaperone activity of α-crystallin. The kinetics of aggregation were monitored by measuring the light scattering of the samples at 360 nm for 120 min. α-Crystallin was preincubated with peptides separately for 1 h in 37 °C before the chaperone activity assay: (1) ADH (150 μg), (2) ADH (150 μg) with α-crystallin (50 μg), (3) ADH (150 μg) with α-crystallin (50 μg) and αA43−56 (5 μg), (4) ADH (150 μg) with α-crystallin (50 μg) and αA43−56 (15 μg), (5) ADH (150 μg) with α-crystallin (50 μg) and αA66−80 (5 μg), and (6) ADH (150 μg) with α-crystallin (50 μg) and αA66−80 (15 μg). The inset shows the SDS−PAGE analysis. Lanes 1−6 contained precipitates of chaperone assay samples 1−6. Samples containing the αA66−80 peptide (lanes 5 and 6) have more precipitated α-crystallin, ADH substrate, and peptide than samples containing the αA43−56 peptide (lanes 3 and 4).

experimental conditions (data not shown). SDS−PAGE analysis of the samples after the chaperone assay (Figure 2, inset) revealed that the samples containing control peptide αA43−56 (Figure 2, inset, lanes 3 and 4) had less ADH substrate and α-crystallin in the pellets than the samples containing the αA66−80 peptide (Figure 2, inset, lanes 5 and 6). Samples that contained the αA66−80 peptide had significantly more precipitation of α-crystallin (20 kDa bands), ADH substrate, and αA66−80 peptide in the pellets. The data suggest that the αA66−80 peptide facilitates the aggregation of α-crystallin and suppresses its chaperone activity. The interaction of the peptide with α-crystallin or with the α-crystallin−ADH complex might be responsible for the enhanced aggregation and increased light scattering. These data suggest that α-crystallin is incorporated into larger aggregates composed of α-crystallin, ADH, and the peptide.

The αA66−80 Peptide Facilitates α-Crystallin Aggregation. To investigate whether α-crystallins incubated with the αA66−80 peptide are more prone to aggregate, the turbidity of the samples was monitored spectrophotometrically by measuring the change in absorbance at 360 nm. When incubated with αA66−80, α-crystallin showed a progressive increase in turbidity during an incubation from 0 to 300 min. Under the same conditions, the control α-crystallin and the αA66−80 peptide alone did not show an increase in turbidity, indicating that the peptide is causing the turbidity in the α-crystallin solution (Figure 3A). The solubility of α-crystallin decreased as the duration of the incubation with the peptide increased (Figure 3B), thus confirming the influence of αA66−80 on turbidity. The peptide-mediated aggregation is also evidenced by the precipitation of α-crystallins, as confirmed by SDS−PAGE analysis (Figure 3C). The α-crystallin used in the study contained 12 and 17 kDa polypeptides as minor contaminants.

dx.doi.org/10.1021/bi301662w | Biochemistry 2013, 52, 3638−3650

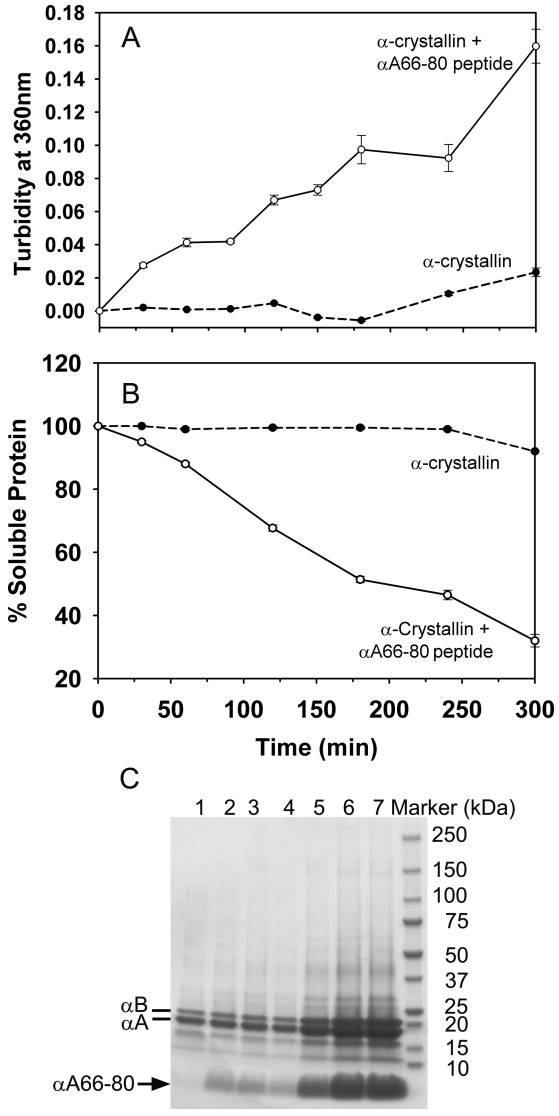

Figure 3. αA66−80-induced aggregation of α-crystallin. (A) α-Crystallin (5 μM) incubated with αA66−80 (25 μM) in 1 mL of 50 mM phosphate buffer monitored at 360 nm with different durations of incubation (data presented as means ± SD of three independent measurements). (B) Concentrations of soluble proteins at different time points during incubation (data represented as means ± SD of three independent measurements). (C) SDS−PAGE analysis. α-Crystallin (10 μM) was incubated with different concentrations of αA66−80 (1.25−20 μM) in 1 mL of 50 mM phosphate buffer (pH 7.2) at 37 °C for 24 h. After incubation, samples were centrifuged at 8000 rpm for 15 min and pellets were dissolved in SDS−PAGE sample buffer and run in a 4 to 20% gel at α-crystallin:αA66−80 ratios of 1:0 (lane 1), 1:0.125 (lane 2), 1:0.25 (lane 3), 1:0.5 (lane 4), 1:1 (lane 5), 1:1.5 (lane 6), and 1:2 (lane 7).

However, these impurities by themselves did not contribute to the aggregation of α-crystallin, because the incubation of the crystallin fraction by itself did not result in appreciable precipitation (Figure 3C, lane 1), whereas the α-crystallin fraction containing an increasing concentration of the αA66−80 peptide showed significant precipitation of proteins (Figure 3C, lanes 5−7). This indicates that α66−80 was primarily responsible for the aggregation and precipitation of α-crystallins. Precipitation seems to be more prominent when the crystallin:peptide ratio is 1:1, 1:1.5, and 1:2 (lanes 5−7, respectively). Thus, an α-crystallin:αA66−80 peptide ratio of at least 1:1 may be the critical concentration required for precipitation. Thus, the presence of the αA66−80 peptide and α-crystallin together in the aggregates correlates with the *in vivo* accumulation of the peptide in water-insoluble aggregates[19] and points to α-crystallin being a major component in cataractous inclusions.[8] The intrinsic tryptophan fluorescence was measured to investigate the effect of the peptide on the α-crystallin conformation. α-Crystallin subunits have three tryptophan residues (position 9 in αA-crystallin and positions 9 and 60 in αB-crystallin), whereas the peptide has no tryptophan residues. Therefore, the fluorescence emission of α-crystallin was monitored in the presence and absence of the αA66−80 peptide to evaluate the change in tryptophan fluorescence following the binding of the peptide to α-crystallin. Native α-crystallin showed emission maxima at 339 nm when it was excited at 295 nm. Emission spectra of α-crystallin mixed with the αA66−80 peptide showed a decrease in the fluorescence intensity with an increasing peptide concentration (Figure 4A). However, there was no shift in the emission maximum. These results suggest the possible association of the peptide with the protein and quenching of the tryptophan emission caused by peptide-induced aggregation. Because there are no available binding models under such aggregating conditions, no meaningful K_d could be deduced from our intrinsic fluorescence measurements. Aggregation of α-crystallin in the presence of the αA66−80 peptide was also evident from our CD (Figure 4B) and SEC (Figure 4C) studies. The far-UV spectrum of the control α-crystallin sample showed a minimum at 218 nm, consistent with previously published results.[33] In α-crystallin samples incubated with the αA66−80 peptide, the spectra did not change, but the CD signal intensity decreased with an increased αA66−80 peptide concentration. The decrease in the magnitude of the CD signal is probably a consequence of aggregate formation, which eventually causes precipitation and loss of the signal (Figure 4B). SEC elution profiles demonstrated no additional soluble aggregate peaks of α-crystallin at any of the peptide concentrations. However, the α-crystallin oligomer showed reduced peak intensity in association with an increased αA66−80 concentration, indicating the formation of insoluble aggregates that are held up by precolumn filters in SEC (Figure 4C).

αA66−80 Peptide Interaction Increases the Surface Hydrophobicity of α-Crystallin. The hallmark of aggregating proteins is their exposed hydrophobic groups.[13] Therefore, to determine if a concomitant change in hydrophobicity occurs during peptide binding, bis-ANS binding experiments were performed. Figure 5 illustrates the emission spectra of α-crystallin in the presence and absence of the peptide. The fluorescence intensity of bis-ANS in α-crystallin samples gradually increased in the presence of increasing concentrations of the αA66−80 peptide, indicating the increased availability of hydrophobic sites on α-crystallin upon interaction with the peptide.

Noncovalent Interactions Stabilize α-Crystallin−αA66−80 Complexes. We have shown that the αA66−80 peptide is able to promote aggregation of α-crystallin. The characteristics of the α-crystallin−αA66−80 aggregate were examined by studying the effects of dissociating agents, including SDS, NaCl, GdmCl, and urea, on the peptide-induced α-crystallin aggregates. The α-crystallin−αA66−80 aggregates were resistant to dissociation (solubilization) by high-ionic strength buffers that contained 1 M NaCl and 2 M

dx.doi.org/10.1021/bi301662w | *Biochemistry* 2013, 52, 3638−3650

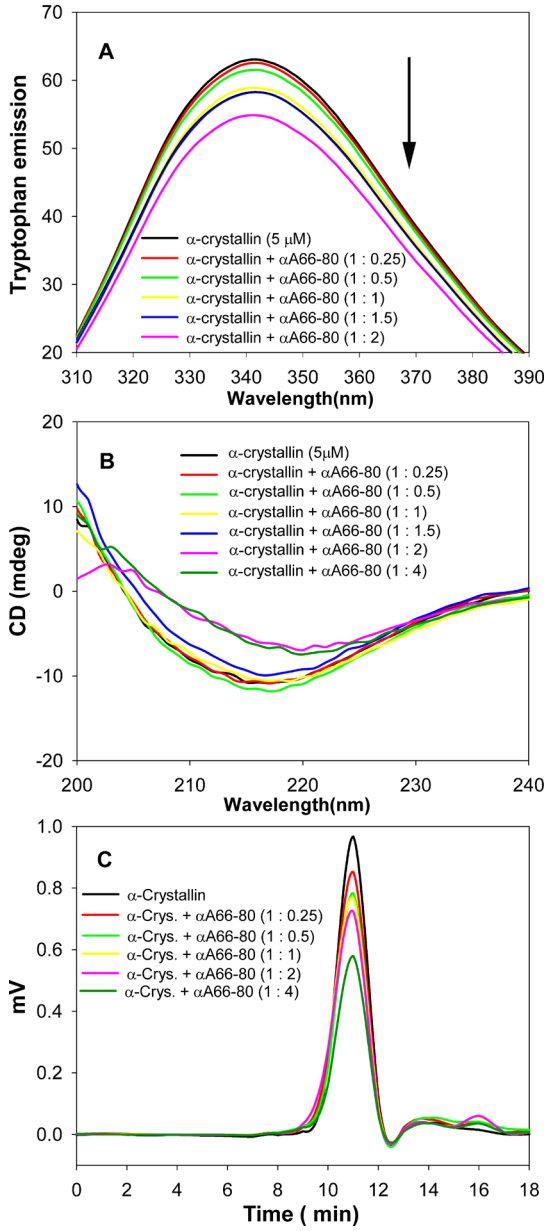

Figure 4. Interaction between α-crystallin and the αA66−80 peptide. (A) Tryptophan fluorescence measurements. The arrow points to the decrease in the intrinsic tryptophan fluorescence of α-crystallin in the presence of increasing peptide concentrations. (B) Far-UV CD spectra. The signal intensity decreases in a manner concomitant with the formation of the insoluble precipitate. (C) Size exclusion chromatography. Chromatograms represent the decrease in the soluble α-crystallin fraction in the presence of αA66−80.

$MgCl_2$ and were only partially affected by PBS and Triton X-100. The maximal solubility (~62−68%) of the α-crystallin and peptide from the aggregates was observed in the presence of strong dissociating agents, urea and GdmCl (Table 1). This suggests that the noncovalent interactions stabilize the peptide−crystallin associations and contribute to the aggregation. These data, combined with the bis-ANS binding studies, indicate that intermolecular hydrophobic interactions play a crucial role in the peptide-mediated α-crystallin aggregation.

Site-Specific Interaction between αA66−80 and αB-Crystallin. Our previous studies showed that the αA66−80 peptide brings about preferential insolubilization of α-crystallin

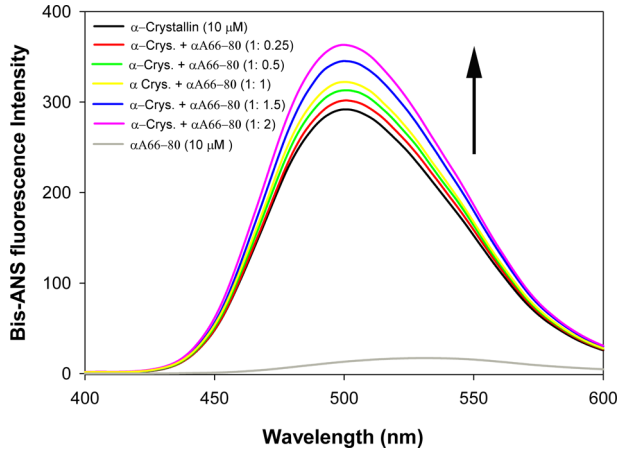

Figure 5. Changes in the surface hydrophobicity of α-crystallin in the presence of the peptide. Emission spectrum of bis-ANS (20 μM) samples bound to α-crystallin in the presence and absence of the αA66−80 peptide. The arrow indicates a gradual increase in bis-ANS fluorescence intensity bound to α-crystallin with an increase in the αA66−80 peptide concentration.

Table 1. Stabilities of the Peptide−Protein Complexes in Dissociating Agents[a]

dissociating agent	protein recovered in the soluble fraction (% of total)[b]
phosphate buffer (PBS)	0.01
PBS with 1% Tween 20	0.012
PBS with 1% Triton X-100	12
1 M NaCl	0.001
2 M $MgCl_2$	0.001
8 M urea	**62**
1% SDS	12
6 M guanidinium hydrochloride	**68**

[a] α-Crystallin and the αA66−80 peptide [2:1 ratio (w/w)] were incubated at 37 °C for 18 h. After incubation, the samples were centrifuged (10000*g* for 10 min), and the aggregates were resuspended in different dissociating agents and placed in roller shaker at 37 °C for 1 h. The samples were again centrifuged at 8000 rpm for 10 min. The protein content of the supernatant was estimated by the Bio-Rad protein assay. The protein content of the sample before the incubation was taken to be 100%. [b] Boldface percentages indicate the maximal solubility of the aggregate in 8 M urea and 6 M guanidinium hydrochloride.

from soluble lens extracts.[19] The preferential insolubilization could be mediated by a specific interaction between the peptide and α-crystallin. To examine the interaction, we used a chemical cross-linking and mass spectrometry approach. In our experiments with α-crystallin, the αA66−80 peptide induced aggregation and precipitation of both αA- and αB-crystallin. To minimize the complexity of analyzing the large number of the peptides in mass spectra arising from both αA- and αB-crystallin subunits, we focused on studying the interaction between αA66−80 and αB-crystallin by using a novel cross-linking reagent. Figure 6 depicts a schematic overview of the analytical strategy we formulated. A biotinylated αA66−80 peptide was used in our experiments to allow detection of the αB-crystallin−peptide complex in gels. The presence of biotin did not affect the interaction between the peptide and αB-crystallin. We used isotope-labeled homobifunctional NHS ester (*N*-hydroxysuccinimide)-BS^2G-

dx.doi.org/10.1021/bi301662w | *Biochemistry* 2013, 52, 3638−3650

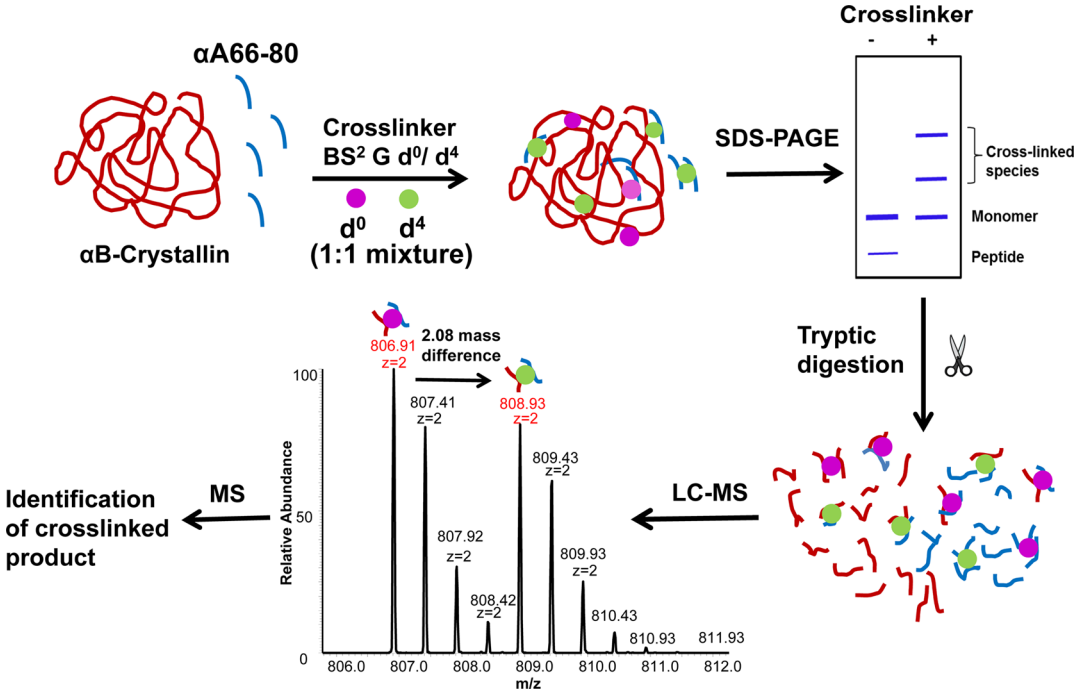

Figure 6. General analytical strategy for the identification of the αA66−80 peptide interaction site in αB-crystallin using a mixture of isotope-labeled and unlabeled cross-linker (BS^2G-d_0 and -d_4).

d_0 or -d_4 [bis(sulfosuccinimidyl) glutarate] cross-linker to examine the peptide interaction site in αB-crystallin (Figure 7A). Homobifunctional cross-linking reagents contain two identical functional groups on either side of the molecule that are separated by a spacer bridging a defined distance. NHS esters are highly reactive toward primary amines (i.e., ε-amino groups of lysines and the free N-terminus of a protein) but less reactive with hydroxyl groups of serine and threonine side chains.[34] Upon cross-linking, NHS esters created amide bonds in peptides that resulted in mass increases of 96.021 and 100.045 with BS^2G-d_0 and BS^2G-d_4, respectively. BS^2G was used in 1:1 mixtures of their deuterated and nondeuterated species to facilitate identification of cross-linked products by means of their distinct doublet isotope patterns with mass differences of 4.025 (d_0 vs d_4) for monoprotonated forms in the deconvoluted mass spectra.[35] BS^2G was employed in a 20-fold molar excess and allowed to react for 45 min in ice, an adequate condition for the formation of a cross-linked complex between αB-crystallin and the peptide without aggregation. The presence of the αB-crystallin−αA66−80 peptide cross-linked complex was detected by Western blot analysis of the SDS−PAGE gel using avidin-HRP that binds to the biotin tag in the peptide. We observed avidin reactivity only in the sample in which the peptide was cross-linked to αB-crystallin (Figure 7B, lane 4). The cross-linked species migrated as two distinct bands, a trace band at 22 kDa and a strong dimer band at 44 kDa in SDS−PAGE, indicating the formation of a well-defined cross-linked complex. The cross-linked species from the 22 kDa band was excised and subsequently used in enzymatic in gel digestion with trypsin.

Nano-MS analysis of tryptic peptides of cross-linked products from gel bands generated numerous peptide signals. The deconvoluted peak lists from LC−MS data, when compared with theoretical mass lists generated by GPMAW (as described in Materials and Methods), revealed five inter-cross-linked species between αB-WT and the αA66−80 peptide from the tryptic peptides of the 22 kDa band (Table 2). Of the five inter-cross-linked pairs identified via LC−MS, two (identified by boldface in Table 2) were confirmed by MS/MS (Figure 8 and Figure S1 of the Supporting Information). Figure 8A gives the LC−MS spectra of the intermolecular cross-linked peptide pair 1612.82/1616.84 [MH^+], which appears as doubly protonated 806.91/808.93 [M_2H^+] ion pairs with a mass difference of 2.02 Da. The identified parent ion was subjected to MS/MS analysis. Figure 8B shows the CID and HCD spectrum with a series of y-type and b-type ions observed. Fragmentation pattern analysis in MS/MS led to the identification of a cross-link between Lys166 in αB-WT and the amino group in the N-terminal serine of the αA66−80 peptide. The cross-link product has the C-terminal region of αB-WT (amino acids 164−174) attached to the αA66−80 peptide (amino acids 66−68) (Figure 8C). The fragmentation pattern of a triply charged ion pair having a mass difference of 1.34 (m/z 622.34/623.68) is shown in Figure S1B of the Supporting Information. The pair corresponds to the cross-linked site between αB-WT (amino acids 91−103) and the αA66−80 peptide (amino acids 66−68) (Figure S1C of the Supporting Information). The other three presumptive cross-links identified (Figure S2 of the Supporting Information) were not sufficiently abundant to perform MS/MS analysis. Figure 9 illustrates the potential αA66−80 interacting sites in αB-crystallin identified by GPMAW from the LC−MS data of the cross-linked band.

To confirm that the interaction of the αA66−80 peptide at the C-terminal extension of αB-crystallin is a specific interaction and not a random interaction, we used αB-crystallin C-terminal peptide 164−174 (αB-CTP) to titrate αA66−80 and measured the changes in the surface hydrophobicity of α-crystallin with bis-ANS. As a control, we used a proline-substituted αA66−80 peptide that does not interact with α-crystallin. The results are shown in Figure S3 of the Supporting Information. The addition of the αA66−80 peptide or αB-CTP

dx.doi.org/10.1021/bi301662w | *Biochemistry* 2013, 52, 3638−3650

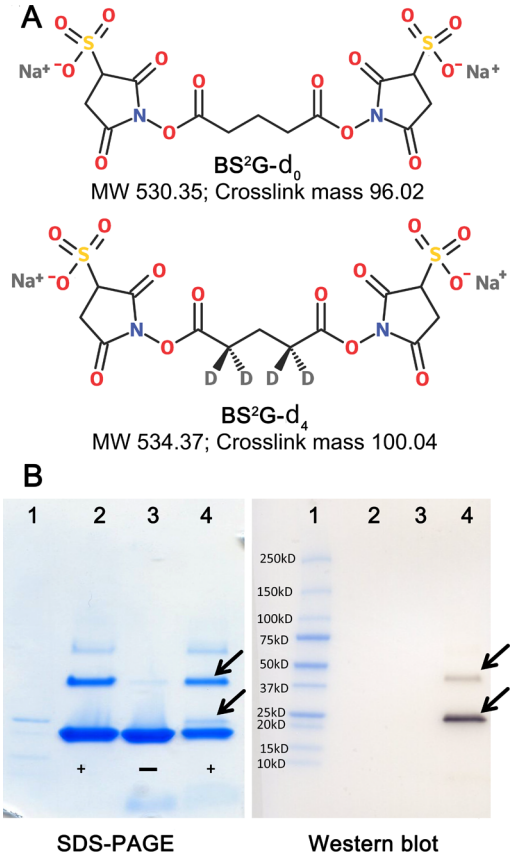

Figure 7. (A) Chemical structures of amine-reactive, homobifunctional, and isotope-labeled (d_0 and d_4) cross-linking reagent BS^{2}G, bis(sulfosuccinimidyl) glutarate. The corresponding mass shifts associated with d_0 and d_4 cross-linked peptides are shown. (B) SDS−PAGE and Western blot of cross-linked αB-crystallin and the biotinylated αA66−80 peptide. The reaction was conducted as described in Materials and Methods with a 20-fold molar excess of cross-linker for 45 min. SDS−PAGE and Western blot: lane 1, marker; lane 2, αBWT control with cross-linker (without peptide); lane 3, αBWT and biotin-αA66−80 without cross-linker; lane 4, αBWT and biotin-αA66−80 with cross-linker. Arrows in the SDS−PAGE gel point to cross-linked complexes containing the biotin-labeled peptide confirmed by Western blots of the gel.

increased the surface hydrophobicity of α-crystallin, whereas the proline-substituted αA66−80 did not. The presence of both αB-CTP and αA66−80 peptides in the sample resulted in no additional increase in the surface hydrophobicity of α-crystallin. These observations suggest that interaction between αB-CTP and the αA66−80 peptide prevents the αA66−80 peptide from binding to α-crystallin (Figure S3 of the Supporting Information). Thus, the cross-linking and dissociation studies together suggest that the αA66−80 peptide binds at multiple sites and forms a tight complex with αB-crystallin.

DISCUSSION

High-molecular weight (HMW) aggregates composed of native, modified, and truncated proteins and peptide fragments are the hallmark of aging and cataract lenses.[1,7,11,12,15] Recent evidence points to the involvement of crystallin fragments in the aggregation of lens proteins.[19] The amyloidogenic αA66−80 peptide is known to progressively accumulate in the water-insoluble aggregates of the aging lens,[12,19] and the peptide preferentially insolubilizes α-crystallin from the soluble lens fractions.[19] However, it is not clear how the peptide influences the structure and function of soluble α-crystallins. Because α-crystallins constitute the major protein in the water-insoluble cataract aggregates, it is important to determine the nature of the interactions between the peptide and α-crystallins. The aims of this study were to identify the sites at which the αA66−80 peptide binds to α-crystallin and the mechanism by which it induces aggregation of soluble α-crystallins. We present here the first evidence of a striking potential of the αA66−80 peptide to form a stable complex with α-crystallin and induce α-crystallin aggregation.

Impact of the αA66−80 Peptide on α-Crystallin. The αA66−80 peptide is localized and concentrated in the nuclear region of the lens.[12,19] In aged human lenses (>70 years old), the concentration of the αA66−80 peptide is 2.33 ± 0.6 nmol/g of lens tissue, and almost all of this is in the nuclear region.[19] In addition, the lens also contains additional peptides that are capable of inducing aggregation of α-crystallin.[11,12,19] In our experiments, we used peptide concentrations in the micromolar range. Such use of high levels of peptide as part of *in vitro* experiments to demonstrate the *in vivo* effect of the peptide has been explained previously.[19,36] The *in vivo* process of cataract pathogenesis and the associated accumulation of peptides take place in a span of years to decades, whereas the time frame of

Table 2. Identification of Potential αB-Crystallin and αA66−80 Cross-Link Pairs from the LC−MS Data Using GPMAW[a]

observed mass pairs [MH$^+$]	intensity	actual mass [MH$^+$]	αB-crystallin sequence	αA66−80 sequence	type	delta	ppm
1612.820	**161427**	**1612.818**	**164−174**	**1−3**	**X-link**	**-0.002**	**−1**
1616.843	**189204**						
1979.082	484245	1979.085	70−74	4−13	X-link	0.003	1
1983.106	703659						
2361.165	1337170	2361.172	75−90	1−3	X-link	0.007	3
2365.192	1336468						
2189.084	206855	2189.095	93−107	1−3	X-link	0.011	5
2193.114	229689						
1865.009	**342231**	**1865.013**	**91−103**	**1−3**	**X-link**	**0.004**	**2**
1869.034	**596374**						

[a]The deconvoluted peak lists from MS spectra were compared with theoretically generated cross-linked peptide masses. The theoretical peak lists were generated using GPMAW. The table gives the observed mass in the LC−MS data, the actual mass (theoretical) generated by GPMAW, and the amino acid segments in the interacting partners. delta corresponds to deviation in mass between the observed and actual masses. Mass pairs and the corresponding cross-linked sites shown in boldface were confirmed by MS/MS.

dx.doi.org/10.1021/bi301662w | *Biochemistry* 2013, 52, 3638−3650

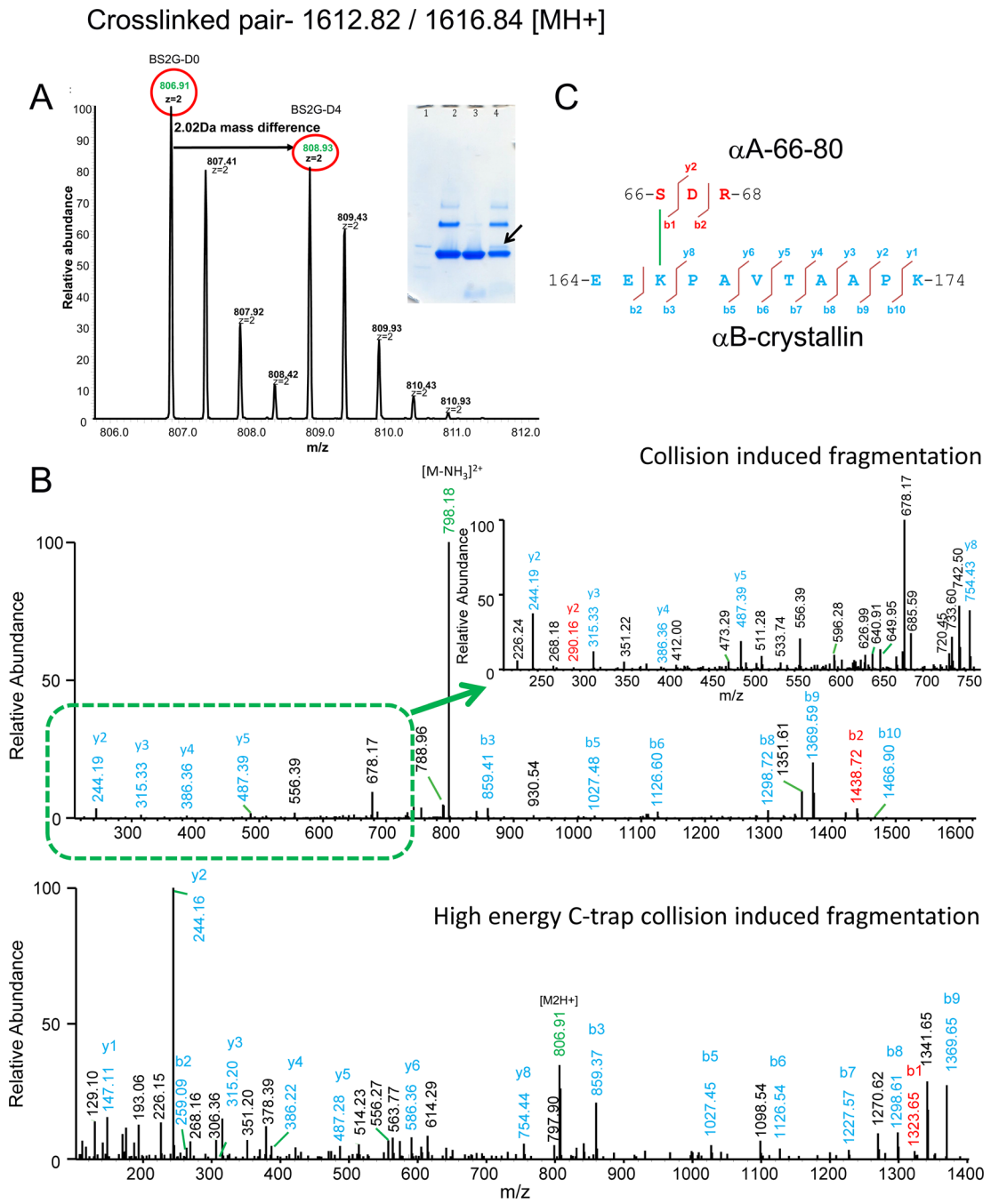

Figure 8. Nano-LC-LTQ Orbitrap identification of the interaction of the αA66−80 peptide with the C-terminal extension of αB-crystallin. (A) Extracted ion chromatogram of the tryptic digest of the cross-linked complex. The signal of doubly charged peptides with ions at *m*/*z* 806.91 and 808.93, cross-linked with light (d_0) and heavy (d_4) precursor ions presenting a mass difference of 2.02 Da, is indicated by an arrow. Inset in A is the SDS−PAGE shown in Figure 7B. (B) Fragmentation mass spectrum (both CID and HCD) of the identified precursor ion (*m*/*z* 806.9) obtained using MS/MS. The identified y- and b-type ions are indicated. (C) Interacting region of the N-terminal amino group of residue 66 of αA66−80 with Lys166 of αB-crystallin shown in the identified cross-linked sequences.

the *in vitro* experiments is limited. Further, the effective concentration of the αA66−80 peptide in the lens could be increased by its interaction with other lens components and by factors like crowding and nuclear localization of most of the peptides. In the presence of αA66−80, α-crystallin has diminished chaperone activity and aggregates into the insoluble form (Figures 2 and 3). Thus, the age-related insolubility of α-crystallin specifically observed in the nuclear region of the lens and the predominant presence of α-crystallin in the water-insoluble aggregates of the lens, which has been known for years, can be attributed to the interactions between the peptide and soluble α-crystallins.

Rapid aggregation of soluble proteins can be caused by self-association of proteins (which might be accompanied by subtle conformational changes),[37] leading to the formation of small oligomers or HMW soluble or insoluble aggregates[38−40] as a result of interactions with peptides and small molecules.[41−44] Our data provide the evidence that supports this phenomenon. First, the quenching of the tryptophan fluorescence of α-crystallin by the peptide suggests that the microenvironment of

dx.doi.org/10.1021/bi301662w | *Biochemistry* 2013, 52, 3638−3650

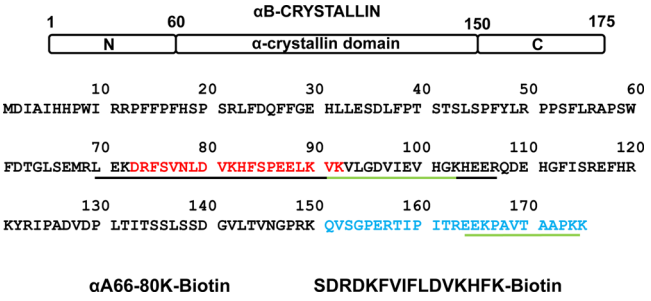

Figure 9. Amino acid sequences of αB-crystallin and biotin-αA66−80 (SDRDKFVIFLDVKHFK-biotin). The blue sequence denotes the C-terminal extension (residues 151−175) in αB-crystallin. The red sequence denotes the chaperone site in αB-crystallin. The underlined sequences in αB-crystallin are presumptive peptide interaction regions identified by GPMAW from the LC−MS data. Sequences underlined in green were confirmed by MS/MS.

intrinsic tryptophan residues in α-crystallin is altered as a consequence of peptide binding. A steady decrease in the tryptophan emission intensity, with no change in the emission maximum, in samples containing the αA66−80 peptide could also indicate a compactness of the tertiary structure or the formation of aggregates.[45−47]

Second, α-crystallin samples incubated with the αA66−80 peptide exhibited reduced peak/signal intensity in our SEC and CD experiments (Figure 4). The decrease in the fluorescence intensity and the magnitude of the CD signal, coupled with the reduction in peak intensity in SEC measurements, suggests that the peptide-induced α-crystallin aggregates are insoluble and hence are lost as precipitates. Such aggregation behavior is due to rapid HMW aggregate formation and precipitation, resulting in particle formation with no detectable intermediates.[45,48]

Third, the bis-ANS signal intensity of α-crystallin was enhanced in the presence of the αA66−80 peptide, demonstrating a conformational change and exposure of hydrophobic residues. This finding correlates well with earlier studies that demonstrated that HMW aggregates in aged and cataract lenses result from exposure of buried β-pleated sheets and an increased number of hydrophobic interactions.[49,50] In both intrinsic tryptophan fluorescence measurement and bis-ANS binding experiments, we did not see any shift in the emission maximum. Tryptophan fluorescence quenching with no shift in the emission maximum under the conditions of aggregation has been reported previously.[46,51] The increase in bis-ANS intensity with no shift in the emission maximum has been observed for mutant crystallin associated with congenital cataract.[52] The apolarity implied in our bis-ANS studies is also relatively small when compared to the large increase in bis-ANS intensity seen in "molten globule" forms where the tertiary structure is substantially disturbed.[53] We therefore conclude that the marked aggregation of α-crystallin by the peptide occurs through minor structural alterations.

The peptide−α-crystallin complexes are stabilized by strong noncovalent interactions because they are partially disrupted and dissociated only by chaotropic agents (6 M GdmCl and 8 M urea) (Table 1), agents known to solubilize amyloid cores in Alzheimer's brain.[54] We were unable to achieve 100% solubilization of aggregates in the presence of urea and GdmCl. At this time, we do not know the reasons for this. A myriad of such noncovalent interactions govern the stability of amyloidal and other protein aggregates in neurodegenerative diseases, suggesting a mechanistic similarity among the disease-causing peptides. Such interactions have been shown to enhance the rate of aggregation and have been identified in the process of both physiological and pathological aggregation of proteins.[38]

Peptides have specific interaction sites on crystallins.[18,55] Using isotope-labeled cross-linking and mass spectrometry, we identified residues 70−74, 75−90, 91−103, 93−107, and 164−174 of αB-crystallin as specific αA66−80 peptide interaction sites (Figure 9). These regions in αB-crystallin are important for their oligomerization, chaperone function, and solubility. In earlier studies, we found that residues 73−92 of αB-crystallin are involved in chaperone function.[56,57] The flexible C-terminal extension of αB-crystallin (residues 164−175) is shown to be important in the solubility, chaperone activity, and oligomeric assembly of the α-crystallin molecule.[58−60] Other identified interaction sites are important for the chaperone ability and subunit interaction.[59] Thus, the peptide interaction at the C-terminal extension, chaperone site, and subunit interaction site might have led to decreased flexibility and diminished chaperone ability, affecting oligomerization and resulting in the decreased solubilization potential of α-crystallin.

Mechanism of αA66−80 Peptide-Induced Aggregation. On the basis of our results, we hypothesize that peptide-

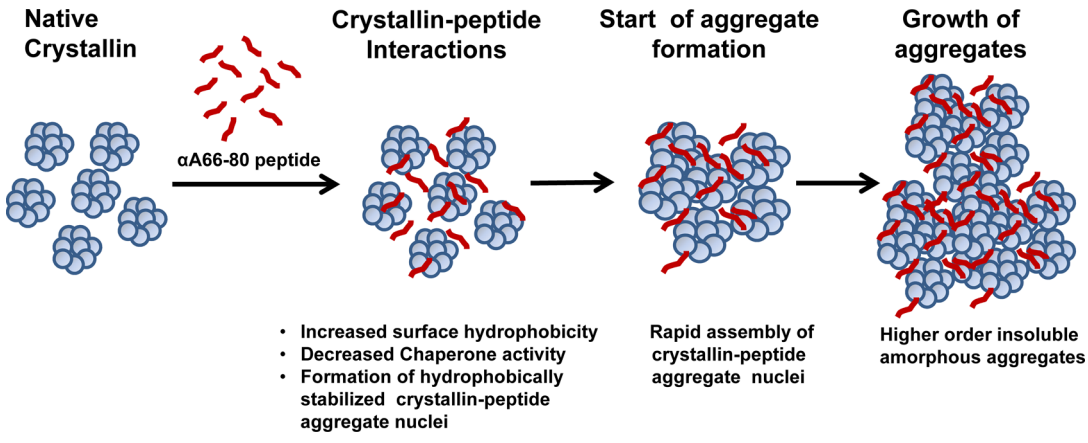

Figure 10. Proposed mechanism of peptide-induced aggregation of soluble crystallins. Stable noncovalent interactions between the αA66−80 peptide and crystallins increase the surface hydrophobicity and facilitate the formation of aggregation nuclei. The rapid assembly of nuclei with soluble crystallins favors formation of large aggregates.

dx.doi.org/10.1021/bi301662w | Biochemistry 2013, 52, 3638−3650

induced crystallin aggregation occurs through the following mechanisms. Binding of the peptide to α-crystallin results in decreased solubility and increased surface hydrophobicity. This acts as the key trigger in the self-association and/or aggregation of protein−peptide complexes into HMW aggregates stabilized by noncovalent interactions. Many such hydrophobic site-mediated nuclei then coalesce together, and the size of the aggregates increases (Figure 10). This view is supported by our time-lapse microscopic recordings that show the formation and growth of HMW aggregates from the nucleus of the α-crystallin−αA66−80 complex.[19] The events may prevent the association of α-crystallin with a denatured substrate and thus suppress α-crystallin chaperone activity (Figure 2) and allow accumulation of unchaperoned, misfolded proteins and their aggregation. In support of this mechanism are our chaperone assays that demonstrated the appearance of the peptide, substrate, and α-crystallin chaperone as insoluble complexes in the aggregate pellet (Figure 2, inset). Thus, the peptide-mediated interactions alter the conformational characteristics and facilitate the aggregation of α-crystallin. Such aggregation and insolubilization of soluble proteins by peptides with amyloidogenic potential have been reported previously.[23,24,46]

Biological Relevance of Peptide-Induced Aggregation. The data presented here, combined with our previous work, provide strong support for the hypothesis that interactions of the peptide with soluble crystallins may be an important contributor in inducing or facilitating protein aggregation and cataract formation. We have developed a model that places the interaction of the peptide and α-crystallin in the context of protein aggregation and cataract formation. The aggregation behavior of proteins is influenced by their solution environment and their stability in the native state.[13] In aging lenses, the solution environment is significantly altered. Slow and progressive degradation of crystallins results in the generation of peptides. The imbalance between the production and clearance of peptides could result in accumulation of the peptide in aging lenses.[7] The accumulating peptides could alter the aggregation behavior of soluble lens proteins as a result of specific interactions with crystallins. Additionally, the interactions may limit the access of these peptides to peptidases, resulting in further accumulation of peptides.

Structural studies of a large number of peptide−protein complexes have shown that the association of peptide with protein causes nonlocal long-range effects. For example, binding of an antigenic peptide to MHC induces conformational changes in the MHC molecule, which in turn facilitates or weakens the binding of other proteins to the MHC molecule.[61] The peptide binding could thus alter the intra- and intermolecular interactions among crystallins. Altered interactions disturb the spatial arrangement of the proteins necessary for lens transparency, which in turn leads to fluctuations in the protein density and refractive index, culminating in increased light scattering.[4] In addition to altering the crystallin−crystallin interactions, the insoluble form of the peptide−protein complex could act as a template for the conversion of soluble components of the lens into the aggregates. The peptides or the peptide−protein complexes may initiate aberrant interactions with other cellular components, resulting in the impairment of cellular function. *In vitro* evidence suggests that these peptides are capable of interacting with membranes as well as modulating crystallin−membrane interactions.[21,62] These protein−peptide aggregates may recruit other proteins and peptides and thus become resistant to degradation or clearance. As with other polymerization reactions, such as those at play in Alzheimer's disease and other tauopathies, peptide fragments in the lens, either alone or in complex with crystallins, could act as a seed for the growth of larger aggregates, consistent with the observation that the peptide fragments are associated with the insoluble aggregates. Thus, a steady accumulation of the LMW peptides initiates a cascade that results in aggregate formation and aggregate growth in the lens, causing an increase in light scattering and leading to loss of vision and cataract. Therefore, mechanisms and strategies for inhibiting peptide generation and peptide interactions could delay or prevent the onset of age-related cataract.

There are several critical questions that remain regarding peptide-induced crystallin aggregation and its relationship to cataract formation. What is the *in vivo* significance of the observed effects that peptides exhibit *in vitro*? In addition to αA66−80, do other peptides with amyloidogenic potential exist in the lens? Do specific peptides make particular contributions to the aggregation of lens proteins? If so, what exactly are the components that form the nucleating complex? What proteases or mechanisms are responsible for the generation of peptides, and why and when are the peptides cleaved from the crystallins during the aging process? Recently, we have identified endogenous proteases in bovine and human lenses with the potential to generate the αA66−80 peptide,[63] and studies of endogenous proteases will likely shed some light on *in vivo* generation of the peptides. To determine whether peptide−crystallin interactions are physiologically significant, the challenge now is to explore in more detail how responses of crystallins to accumulating peptides are coupled to those manifested via other environmental insults. It is of clinical interest that aggregation can be avoided by inhibiting the proteases that generate the peptide fragments. Developing a way to inhibit protease activity may open a novel window to suppress or delay age-related cataract formation.

■ ASSOCIATED CONTENT

Supporting Information

LC−MS and MS/MS spectra of additional cross-linked peptides identified and the data supporting the specific interaction between the αA66−80 peptide and the C-terminal extension of αB-crystallin. This material is available free of charge via the Internet at http://pubs.acs.org.

■ AUTHOR INFORMATION

Corresponding Author

*Department of Ophthalmology, EC213, University of Missouri, One Hospital Drive, Columbia, MO 65212. E-mail: Sharmak@health.missouri.edu. Telephone: (573) 882-8478. Fax: (573) 884-4100.

Funding

Supported by National Institutes of Health Grant EY 019878 and an unrestricted grant-in-aid from Research to Prevent Blindness to the Department of Ophthalmology.

Notes

The authors declare no competing financial interest.

■ ACKNOWLEDGMENTS

We thank Sharon Morey for help in the preparation of the manuscript.

■ ABBREVIATIONS

ADH, alcohol dehydrogenase; HMW, high-molecular weight; LMW, low-molecular weight; WIS, water-insoluble; WS, water-soluble; bis-ANS, 4,4′-bis(1-anilinonaphthalene 8-sulfonate); GdmCl, guanidinium hydrochloride; CD, circular dichroism; SEC, size exclusion chromatography; Aβ, β-amyloid; NHS, *N*-hydroxysuccinimide esters; BS^2G-d_0 and -d_4, nondeuterated and deuterated bis(sulfosuccinimidyl) glutarate, respectively; DMSO, dimethyl sulfoxide; PVDF, polyvinylidene difluoride; HRP, horseradish peroxidase; GPMAW, General Protein Mass Analysis for Windows; CID, collision-induced dissociation; HCD, high-energy C-trap collision-induced dissociation; SD, standard deviation.

■ REFERENCES

(1) Bloemendal, H., de Jong, W., Jaenicke, R., Lubsen, N. H., Slingsby, C., and Tardieu, A. (2004) Ageing and vision: Structure, stability and function of lens crystallins. *Prog. Biophys. Mol. Biol. 86*, 407−485.

(2) Chiti, F., and Dobson, C. M. (2006) Protein misfolding, functional amyloid, and human disease. *Annu. Rev. Biochem. 75*, 333−366.

(3) Horwitz, J. (1992) α-Crystallin can function as a molecular chaperone. *Proc. Natl. Acad. Sci. U.S.A. 89*, 10449−10453.

(4) Takemoto, L., and Sorensen, C. M. (2008) Protein-protein interactions and lens transparency. *Exp. Eye Res. 87*, 496−501.

(5) Hooi, M. Y., and Truscott, R. J. (2011) Racemisation and human cataract. D-Ser, D-Asp/Asn and D-Thr are higher in the lifelong proteins of cataract lenses than in age-matched normal lenses. *Age (Dordrecht, Neth.) 33*, 131−141.

(6) Hains, P. G., and Truscott, R. J. (2007) Post-translational modifications in the nuclear region of young, aged, and cataract human lenses. *J. Proteome Res. 6*, 3935−3943.

(7) Sharma, K. K., and Santhoshkumar, P. (2009) Lens aging: Effects of crystallins. *Biochim. Biophys. Acta 1790*, 1095−1108.

(8) Harrington, V., Srivastava, O. P., and Kirk, M. (2007) Proteomic analysis of water insoluble proteins from normal and cataractous human lenses. *Mol. Vision 13*, 1680−1694.

(9) Grey, A. C., and Schey, K. L. (2009) Age-related changes in the spatial distribution of human lens α-crystallin products by MALDI imaging mass spectrometry. *Invest. Ophthalmol. Visual Sci. 50*, 4319−4329.

(10) Roy, D., and Spector, A. (1978) Human insoluble lens protein. II. Isolation and characterization of a 9600 Da polypeptide. *Exp. Eye Res. 26*, 445−459.

(11) Santhoshkumar, P., Udupa, P., Murugesan, R., and Sharma, K. K. (2008) Significance of interactions of low molecular weight crystallin fragments in lens aging and cataract formation. *J. Biol. Chem. 283*, 8477−8485.

(12) Su, S. P., McArthur, J. D., and Andrew Aquilina, J. (2010) Localization of low molecular weight crystallin peptides in the aging human lens using a MALDI mass spectrometry imaging approach. *Exp. Eye Res. 91*, 97−103.

(13) Stefani, M., and Dobson, C. M. (2003) Protein aggregation and aggregate toxicity: New insights into protein folding, misfolding diseases and biological evolution. *J. Mol. Med. (Heidelberg, Ger.) 81*, 678−699.

(14) Stefani, M. (2012) Structural features and cytotoxicity of amyloid oligomers: Implications in Alzheimer's disease and other diseases with amyloid deposits. *Prog. Neurobiol. 99*, 226−245.

(15) Srivastava, O. P. (1988) Age-related increase in concentration and aggregation of degraded polypeptides in human lenses. *Exp. Eye Res. 47*, 525−543.

(16) Harrington, V., McCall, S., Huynh, S., Srivastava, K., and Srivastava, O. P. (2004) Crystallins in water soluble-high molecular weight protein fractions and water insoluble protein fractions in aging and cataractous human lenses. *Mol. Vision 10*, 476−489.

(17) Surolia, I., Sinha, S., Sarkar, D. P., Reddy, P. Y., Reddy, G. B., and Surolia, A. (2008) Concurrence of Danish dementia and cataract: Insights from the interactions of dementia associated peptides with eye lens α-crystallin. *PLoS One 3*, e2927.

(18) Udupa, E. G., and Sharma, K. K. (2005) Effect of oxidized βB3-crystallin peptide on lens βL-crystallin: Interaction with βB2-crystallin. *Invest. Ophthalmol. Visual Sci. 46*, 2514−2521.

(19) Santhoshkumar, P., Raju, M., and Sharma, K. K. (2011) αA-Crystallin peptide SDRDKFVIFLDVKHF accumulating in aging lens impairs the function of α-crystallin and induces lens protein aggregation. *PLoS One 6*, e19291.

(20) Su, S. P., McArthur, J. D., Truscott, R. J., and Aquilina, J. A. (2011) Truncation, cross-linking and interaction of crystallins and intermediate filament proteins in the aging human lens. *Biochim. Biophys. Acta 1814*, 647−656.

(21) Su, S. P., McArthur, J. D., Friedrich, M. G., Truscott, R. J., and Aquilina, J. A. (2011) Understanding the α-crystallin cell membrane conjunction. *Mol. Vision 17*, 2798−2807.

(22) Srivastava, O. P., and Srivastava, K. (2012) In-vivo existing human lens crystallin fragments form amyloid-type aggregates in vitro. ARVO 53, E-Abstract 2278.

(23) Konno, T. (2001) Amyloid-induced aggregation and precipitation of soluble proteins: An electrostatic contribution of the Alzheimer's β(25−35) amyloid fibril. *Biochemistry 40*, 2148−2154.

(24) Olzscha, H., Schermann, S. M., Woerner, A. C., Pinkert, S., Hecht, M. H., Tartaglia, G. G., Vendruscolo, M., Hayer-Hartl, M., Hartl, F. U., and Vabulas, R. M. (2011) Amyloid-like aggregates sequester numerous metastable proteins with essential cellular functions. *Cell 144*, 67−78.

(25) Sharma, K. K., Kumar, R. S., Kumar, G. S., and Quinn, P. T. (2000) Synthesis and characterization of a peptide identified as a functional element in αA-crystallin. *J. Biol. Chem. 275*, 3767−3771.

(26) Santhoshkumar, P., and Sharma, K. K. (2004) Inhibition of amyloid fibrillogenesis and toxicity by a peptide chaperone. *Mol. Cell. Biochem. 267*, 147−155.

(27) Roy, D., and Spector, A. (1976) Absence of low-molecular-weight α-crystallin in nuclear region of old human lenses. *Proc. Natl. Acad. Sci. U.S.A. 73*, 3484−3487.

(28) Truscott, R. J., and Augusteyn, R. C. (1977) Changes in human lens proteins during nuclear cataract formation. *Exp. Eye Res. 24*, 159−170.

(29) Sharma, K. K., Kaur, H., and Kester, K. (1997) Functional elements in molecular chaperone α-crystallin: Identification of binding sites in αB-crystallin. *Biochem. Biophys. Res. Commun. 239*, 217−222.

(30) Santhoshkumar, P., Murugesan, R., and Sharma, K. K. (2009) Deletion of (54)FLRAPSWF(61) residues decreases the oligomeric size and enhances the chaperone function of αB-crystallin. *Biochemistry 48*, 5066−5073.

(31) Sreelakshmi, Y., Santhoshkumar, P., Bhattacharyya, J., and Sharma, K. K. (2004) αA-Crystallin interacting regions in the small heat shock protein, αB-crystallin. *Biochemistry 43*, 15785−15795.

(32) Sharma, K. K., Kumar, G. S., Murphy, A. S., and Kester, K. (1998) Identification of 1,1′-bi(4-anilino)naphthalene-5,5′-disulfonic acid binding sequences in α-crystallin. *J. Biol. Chem. 273*, 15474−15478.

(33) Raman, B., Ramakrishna, T., and Rao, C. M. (1995) Rapid refolding studies on the chaperone-like α-crystallin. Effect of α-crystallin on refolding of β- and γ-crystallins. *J. Biol. Chem. 270*, 19888−19892.

(34) Madler, S., Bich, C., Touboul, D., and Zenobi, R. (2009) Chemical cross-linking with NHS esters: A systematic study on amino acid reactivities. *J. Mass Spectrom. 44*, 694−706.

(35) Ihling, C., Schmidt, A., Kalkhof, S., Schulz, D. M., Stingl, C., Mechtler, K., Haack, M., Beck-Sickinger, A. G., Cooper, D. M., and Sinz, A. (2006) Isotope-labeled cross-linkers and Fourier transform ion cyclotron resonance mass spectrometry for structural analysis of a protein/peptide complex. *J. Am. Soc. Mass Spectrom. 17*, 1100−1113.

(36) Hu, X., Crick, S. L., Bu, G., Frieden, C., Pappu, R. V., and Lee, J. M. (2009) Amyloid seeds formed by cellular uptake, concentration,

and aggregation of the amyloid-β peptide. *Proc. Natl. Acad. Sci. U.S.A. 106*, 20324−20329.
(37) Rousseau, F., Schymkowitz, J., and Serrano, L. (2006) Protein aggregation and amyloidosis: Confusion of the kinds? *Curr. Opin. Struct. Biol. 16*, 118−126.
(38) Wang, W., Nema, S., and Teagarden, D. (2010) Protein aggregation: Pathways and influencing factors. *Int. J. Pharm. 390*, 89−99.
(39) Weiss, W. F. t., Young, T. M., and Roberts, C. J. (2009) Principles, approaches, and challenges for predicting protein aggregation rates and shelf life. *J. Pharm. Sci. 98*, 1246−1277.
(40) Roberts, C. J. (2007) Non-native protein aggregation kinetics. *Biotechnol. Bioeng. 98*, 927−938.
(41) Uversky, V. N., Li, J., and Fink, A. L. (2001) Metal-triggered structural transformations, aggregation, and fibrillation of human α-synuclein. A possible molecular NK between Parkinson's disease and heavy metal exposure. *J. Biol. Chem. 276*, 44284−44296.
(42) Shalova, I. N., Asryants, R. A., Sholukh, M. V., Saso, L., Kurganov, B. I., Muronetz, V. I., and Izumrudov, V. A. (2005) Interaction of polyanions with basic proteins, 2(a): Influence of complexing polyanions on the thermo-aggregation of oligomeric enzymes. *Macromol. Biosci. 5*, 1184−1192.
(43) Ahn, H. J., Zamolodchikov, D., Cortes-Canteli, M., Norris, E. H., Glickman, J. F., and Strickland, S. (2010) Alzheimer's disease peptide β-amyloid interacts with fibrinogen and induces its oligomerization. *Proc. Natl. Acad. Sci. U.S.A. 107*, 21812−21817.
(44) Artemova, N., Stein-Margolina, V., Smirnova, E., and Gurvits, B. (2012) Formation of supramolecular structures of a native-like protein in the presence of amphiphilic peptides: Variations in aggregate morphology. *FEBS Lett. 586*, 186−190.
(45) Malik, R., and Roy, I. (2011) Probing the mechanism of insulin aggregation during agitation. *Int. J. Pharm. 413*, 73−80.
(46) Artemova, N. V., Stein-Margolina, V. A., Bumagina, Z. M., and Gurvits, B. Y. (2011) Acceleration of protein aggregation by amphiphilic peptides: Transformation of supramolecular structure of the aggregates. *Biotechnol. Prog. 27*, 846−854.
(47) Duy, C., and Fitter, J. (2006) How aggregation and conformational scrambling of unfolded states govern fluorescence emission spectra. *Biophys. J. 90*, 3704−3711.
(48) Golub, N., Meremyanin, A., Markossian, K., Eronina, T., Chebotareva, N., Asryants, R., Muronets, V., and Kurganov, B. (2007) Evidence for the formation of start aggregates as an initial stage of protein aggregation. *FEBS Lett. 581*, 4223−4227.
(49) Fujii, N., Awakura, M., Takemoto, L., Inomata, M., Takata, T., Fujii, N., and Saito, T. (2003) Characterization of αA-crystallin from high molecular weight aggregates in the normal human lens. *Mol. Vision 9*, 315−322.
(50) Liang, J. J., and Akhtar, N. J. (2000) Human lens high-molecular-weight α-crystallin aggregates. *Biochem. Biophys. Res. Commun. 275*, 354−359.
(51) Jiang, W., Han, Y., Zhou, R., Zhang, L., and Liu, C. (2007) DNA is a template for accelerating the aggregation of copper, zinc superoxide dismutase. *Biochemistry 46*, 5911−5923.
(52) Singh, D., Raman, B., Ramakrishna, T., and Rao, Ch. M. (2006) The cataract-causing mutation G98R in human αA-crystallin leads to folding defects and loss of chaperone activity. *Mol. Vision 12*, 1372−1379.
(53) Matulis, D., and Lovrien, R. (1998) 1-Anilino-8-naphthalene sulfonate anion-protein binding depends primarily on ion pair formation. *Biophys. J. 74*, 422−429.
(54) Masters, C. L., Simms, G., Weinman, N. A., Multhaup, G., McDonald, B. L., and Beyreuther, K. (1985) Amyloid plaque core protein in Alzheimer disease and Down syndrome. *Proc. Natl. Acad. Sci. U.S.A. 82*, 4245−4249.
(55) Rao, G., Santhoshkumar, P., and Sharma, K. K. (2008) Anti-chaperone βA3/A1(102−117) peptide interacting sites in human αB-crystallin. *Mol. Vision 14*, 666−674.
(56) Bhattacharyya, J., Padmanabha Udupa, E. G., Wang, J., and Sharma, K. K. (2006) Mini-αB-crystallin: A functional element of αB-crystallin with chaperone-like activity. *Biochemistry 45*, 3069−3076.
(57) Santhoshkumar, P., and Sharma, K. K. (2006) Conserved F84 and P86 residues in αB-crystallin are essential to effectively prevent the aggregation of substrate proteins. *Protein Sci. 15*, 2488−2498.
(58) Smulders, R., Carver, J. A., Lindner, R. A., van Boekel, M. A., Bloemendal, H., and de Jong, W. W. (1996) Immobilization of the C-terminal extension of bovine αA-crystallin reduces chaperone-like activity. *J. Biol. Chem. 271*, 29060−29066.
(59) Pasta, S. Y., Raman, B., Ramakrishna, T., and Rao, Ch. M. (2002) Role of the C-terminal extensions of α-crystallins. Swapping the C-terminal extension of α-crystallin to αB-crystallin results in enhanced chaperone activity. *J. Biol. Chem. 277*, 45821−45828.
(60) Kallur, L. S., Aziz, A., and Abraham, E. C. (2008) C-Terminal truncation affects subunit exchange of human αA-crystallin with αB-crystallin. *Mol. Cell. Biochem. 308*, 85−91.
(61) London, N., Movshovitz-Attias, D., and Schueler-Furman, O. (2010) The structural basis of peptide-protein binding strategies. *Structure 18*, 188−199.
(62) Friedrich, M. G., Lam, J., and Truscott, R. J. (2012) Degradation of an old human protein: Age-dependent cleavage of γS-crystallin generates a peptide that binds to cell membranes. *J. Biol. Chem. 287*, 39012−39020.
(63) Hariharapura, R., Santhoshkumar, P., and Krishna Sharma, K. (2013) Profiling of lens protease involved in generation of αA-66−80 crystallin peptide using an internally quenched protease substrate. *Exp. Eye Res. 109*, 51−59.